Prospects for quarkonia production studies in U + U collisions

Daniel Kikoła, Grazyna Odyniec, and Ramona Vogt

Phys. Rev. C **84**, 054907 — Published 11 November 2011
DOI: 10.1103/PhysRevC.84.054907

Prospects for quarkonia production studies in U+U collisions

Daniel Kikoła[1*], Grazyna Odyniec[1], Ramona Vogt[2,3]
[1]Nuclear Science Division, Lawrence Berkeley National Laboratory, Berkeley, CA 94720
[2]Physics Division, Lawrence Livermore National Laboratory, Livermore, CA 94551
[3]Physics Department, University of California, Davis, California, 95616
(Dated: October 5, 2011)

Collisions of deformed uranium nuclei provide a unique opportunity to study the spatial dependence of charmonium in-medium effects. By selecting the orientations of the colliding nuclei, different path lengths through the nuclear medium could be selected within the same experimental environment. In addition, higher energy densities can be achieved in U+U collisions relative to Au+Au collisions. In this paper, we investigate the prospects for charmonium studies with U+U collisions. We discuss the effects of shadowing and nuclear absorption on the J/ψ yield. We introduce a new observable which could help distinguish between different types of J/ψ interactions in hot and dense matter.

I. INTRODUCTION

Collisions of deformed nuclei, such as ^{238}U, are an interesting alternative to those of more spherical ^{197}Au nuclei at RHIC because changes in the nuclear orientation allow wider variations in energy density within the same system [1–4]. Previously, studies of U+U collisions were discussed in the context of elliptic flow. The quantity v_2/ϵ, where v_2 is the elliptic flow parameter and ϵ is the initial spatial eccentricity, provides valuable information about the matter created in heavy-ion collisions [5]. In a dilute system, v_2/ϵ scales like $1/S_\perp dN_{\rm ch}/dy$, where $dN_{\rm ch}/dy$ is the charged particle density and $S_\perp$ is the transverse area of the overlap zone. In central Au+Au collisions at $\sqrt{s_{_{NN}}} = 200$ GeV v_2/ϵ reaches the limit predicted by ideal hydrodynamics for strongly-interacting matter [6] which can be interpreted as a signature of quark-gluon plasma (QGP) formation. It was argued that U+U interactions could provide higher densities and a larger spatial eccentricity, testing whether v_2/ϵ saturates, as predicted by ideal hydrodynamics, or increases further with $dN_{\rm ch}/dy$ [1, 4, 7].

Charmonium production is another key observable for studying the properties of the hot and dense matter created in relativistic heavy-ion collisions. Some time ago J/ψ suppression was proposed as a signal of QGP formation [8]. The suppression is expected to arise from color screening of the binding potential in a QGP, similar to Debye screening in a classical electromagnetic plasma. The magnitude of the suppression depends on the charmonium binding energy and the energy density of the medium, related to the temperature. Therefore, studies of J/ψ production, particularly at low transverse momenta, reveal the thermodynamic properties of the medium.

The suppression of J/ψ production has been studied in detail at the CERN SPS and at RHIC. The NA50 and NA60 experiments at the CERN SPS, $\sqrt{s_{_{NN}}} = 17.3$ GeV, observed strong J/ψ suppression as a function of collision centrality [9–11]. Results from the PHENIX collaboration at RHIC show that the J/ψ suppression in midrapidity Au+Au collisions at $\sqrt{s_{_{NN}}} = 200$ GeV is similar to that observed at SPS energies [12] even though the energy densities and temperatures reached at RHIC are much higher than those at the SPS. Moreover, the forward rapidity J/ψ suppression at RHIC is stronger than at midrapidity. Such a pattern suggests that either additional processes compensate for the effects of color screening or the suppression has different origins at the two energies.

There are several processes which may affect charmonium production in nucleus-nucleus collisions. For comprehensive reviews of different aspects of quarkonium in-medium interactions, see Refs. [13, 14]. Here we briefly summarize a few relevant features, some of which we address in more detail later.

Suppression by cold nuclear matter (CNM) effects such as parton shadowing and absorption by nuclear matter are very important, although not yet established with satisfactory precision [15]. For example, parameterizations of gluon shadowing differ significantly between models [16]. At RHIC energies, CNM effects are studied in d+Au collisions. Changing the shadowing parametrization can significantly affect the magnitude of the absorption cross section required to match the measured nuclear modification factor $R_{\rm dAu}$. In addition, feed-down from radiative or hadronic decays account for 40-50% of the observed $1S$ quarkonium states (J/ψ and Υ). The higher mass quarkonium states have very different radii and formation times and should thus also have different absorption cross sections. While the experimentally measured ψ' absorption cross section is significantly larger than the J/ψ at fixed-target energies, the difference decreases with increasing $\sqrt{s_{_{NN}}}$ [17, 18]. The energy and A dependence of χ_c absorption is unknown [19]. The importance of absorption for higher bottomonium states is also not known.

---

* Now at Physics Department, Purdue University, West Lafayette, IN 47907

If color screening dominates the J/ψ in-medium interaction, the characteristic pattern of sequential charmonium "melting" should be observed. The binding energies of higher mass charmonium states, ψ' and χ_c, are smaller than the J/ψ. Therefore these states dissociate at lower energy densities compared to J/ψ so that, at higher T their feed-down would no longer contribute to the measured J/ψ yield. The remaining, direct, J/ψ production would be suppressed at larger energy densities. This process would result in a step-like dependence of the J/ψ survival probability as a function of energy density [20]. A similar sequential melting would apply to bottomonium.

Suppression due to interactions with comoving partonic and hadronic matter has also been postulated. The A dependence of comover dissociation is similar to that of nuclear absorption [21, 22]. The effects are generally assumed to be small although they strongly depend on the model [21, 23, 24].

J/ψ production may be also enhanced by statistical coalescence in QGP. In this case, the J/ψ yield, $N^{J/\psi}_{\rm stat}$, is proportional to the square of the number of charm quarks in the system, N_c, so that $N^{J/\psi}_{\rm stat} \propto N_c^2$. The charm yield is expected to be proportional to the number of binary NN collisions, $N_{\rm bin}$, i.e. $N_{c\overline{c}} \propto N_{\rm bin}$. The $c\overline{c}$ production rate is not expected to be modified in the QGP. If the density of charm quarks is high enough, then secondary J/ψ production by coalescence of uncorrelated c and $\overline{c}$ quarks at hadronization can occur [25, 26].

Combinations of the above effects have previously been used to describe the J/ψ data. Despite different assumptions about the initial state of the system, models including cold matter effects together with different combinations of color screening, comover absorption, coalescence give quantitatively similar results at RHIC [27]. It is expected that U+U collisions could provide additional means for distinguishing between these effects.

By selecting particular orientations of U+U collisions, different path lengths through nuclear matter, resulting in different effective nuclear absorption cross sections and available energy densities, could be studied. Interactions with the long axes of U nuclei aligned along the beam ("Tip+Tip" or "TT" configurations) give the highest energy densities as well as the longest path, L, through the matter. In contrast, L is shortest in the configuration where the short axes of the U nuclei are aligned along the beam axis ("Side+Side" or "SS" configurations). Different orientations of U+U interactions could study nuclear absorption with reduced uncertainties due to shadowing, as we will show. In general, U+U interactions provide an additional check on models which describe the Au+Au data because some effects, such as shadowing, should be similar in U+U and Au+Au interactions.

We investigate the feasibility of complementing Au+Au collisions with U+U studies of charmonium production and suppression to distinguish between scenarios of J/ψ in-medium interactions. We also discuss CNM effects in U+U collisions.

II. COMPUTATIONAL FRAMEWORK

Here, we discuss two types of cold nuclear matter effects: nuclear absorption and shadowing. Shadowing, the modification of the parton densities in nuclei relative to free protons, is an initial-state effect. Nuclear absorption, the breakup of the charmonium state as it traverses nuclear matter, is a final-state process. The two effects are assumed to factorize. We neglect interactions with hadronic comovers.

We employ the computational framework for studies of cold nuclear matter effects described in Ref. [28]. The nuclear parton densities, $f_i^A(x, Q^2, \vec{r}_T, z)$, where A is the atomic mass number, $\vec{r}_T$ and z are the transverse and longitudinal location of the parton in position space, x is the parton momentum fraction and Q^2 is the interaction scale, factorize into the nucleon density in the nucleus, $\rho_A(\vec{r}_T, z)$, independent of the kinematics; the nucleon parton density, $f_i^p(x, Q^2)$, independent of A; and a shadowing ratio, $S^i(A, x, Q^2, \vec{r}_T, z)$ that parameterizes the modifications of the nucleon parton densities in the nucleus so that

$$f_i^A(x, Q^2, \vec{r}_T, z) \; = \; \rho_A(\vec{r}_T, z) S^i(A, x, Q^2, \vec{r}_T, z) f_i^p(x, Q^2) \; . \tag{1}$$

The effect of shadowing is stronger in central collisions, while at asymptotic distances shadowing disappears. Averaging over impact parameter, the minimum bias result measured in nuclear deep-inelastic scattering is regained. We use the EPS09 shadowing parametrization [16] and assume that the impact parameter dependence of shadowing is proportional to the local nuclear density [29] and exhibits a relatively sharp transition region around $b \sim 2R_A$, see Fig. 1. If one assumes instead that the impact parameter dependence is proportional to the path length L, S^i exhibits a weaker transition region [30]. We discuss the consequences of different assumptions of this b dependence in the next section. At RHIC energies quarkonium production is dominated by gluon fusion. Therefore, shadowing generally refers to gluon shadowing in this context. We employed the Woods-Saxon density distribution for deformed nuclei [3] to describe $\rho_{\rm U}(\vec{r}_T, z)$,

$$\rho_{\rm U}(\vec{r}_T, z) = \rho_0 (1 + \exp[(r - R_C)/a])^{-1} \tag{2}$$

$$R_C \equiv R_0 (1 + \beta_2 Y_{20} + \beta_4 Y_{40}) \tag{3}$$

where ρ_0 is the density at the center of the nucleus, R_C is the total effective radius, Y_{20} and Y_{40} are Legendre polynomials, dependent on $\cos\theta$, where θ is the polar angle, $\vec{r}_T = (r_T\cos\theta, r_T\sin\theta)$ and $r = \sqrt{|\vec{r}_T|^2 + z^2}$. The deformation parameters are $\beta_2 = 0.28$ and $\beta_4 = 0.093$ with $R_0 = 6.81$ fm and $a = 0.54$ fm. In the SS orientation, $\cos\theta = 0$ and $R_C = R_{\rm S} = 6.41$ fm while in the TT orientation, $\cos\theta = 1$ and $R_C = R_{\rm T} = 8.56$ fm.

To implement nuclear absorption on quarkonium production, the production cross section is weighted by the survival probability, $S_{\rm abs}$,

$$S_{\rm abs}(\vec{b} - \vec{r}_T, z') = \exp\left\{ -\int_{z'}^{\infty} dz'' \rho_A(\vec{b} - \vec{r}_T, z'') \sigma_{\rm abs}(z'' - z') \right\} \tag{4}$$

where z' is the longitudinal production point and z'' is the point at which the state is absorbed. The nucleon absorption cross section, $\sigma_{\rm abs}$, typically depends on the spatial location at which the state is produced and how far it travels through the medium.

III. COLD NUCLEAR MATTER EFFECTS IN U+U COLLISIONS

In this section, we investigate whether it is possible to separate the CNM effects of shadowing and absorption in U+U collisions. Nuclear absorption depends on the nuclear path length L. Therefore, it is expected to be considerably different in the TT and SS orientations of U+U collisions. Since L also depends on the impact parameter, b, the effective magnitude of nuclear absorption also changes with b. The dependence of shadowing on the TT and SS orientations is expected be less significant. Moreover, if the difference between collisions in the TT and SS orientations does not depend (or depends only weakly) on the strength of the shadowing, then the ratio of quarkonium production in TT and SS orientations would be effectively independent of the shadowing parametrization. This would greatly simplify the extraction of absorption effects because the systematic error due to shadowing would be significantly reduced.

We first investigate shadowing and nuclear absorption separately and then discuss the combined intensity of these CNM effects in U+U collisions. In order to estimate the strength of each effect, we compare results in the TT and SS orientations where the difference between the two cases should be most apparent. We assume that it will be possible to select these configurations with an efficiency appropriate for charmonium studies, as discussed later.

We begin with an investigation of the charmonium survival probability in U+U collisions for shadowing alone, $S_{\rm shad}$. Figure 1 shows $S_{\rm shad}$ as a function of b in TT and SS configurations of U+U collisions at $y = 0$ and 1.75, calculated in the color evaporation model of quarkonium production [27]. (We do not show results at backward rapidity since the results are symmetric around $y = 0$ in AA collisions.) Note that $S_{\rm shad} < 1$ represents shadowing, $S_{\rm shad} > 1$ antishadowing, and $S_{\rm shad} = 1$ no shadowing. The convolution of two shadowing parameterizations results in stronger shadowing at midrapidity than at forward rapidity for central EPS09 shadowing, as we show in more detail later. The CEM results exhibit a consistent pattern between shadowing effects at leading and next-to-leading order [15]. This behavior is typical of most shadowing parameterizations based on collinear factorization [31].

Calculations of color singlet J/ψ interactions in the dipole approximation suggest that collinear factorization may be inapplicable due to the coherence of the interaction [32, 33]. In this case, higher-twist effects enhanced by powers of $A^{1/3}$ would dominate pA interactions and enhanced J/ψ suppression should set in at large rapidity. However, such enhanced effects are seen in fixed-target energies as well, outside the range of validity of gluon saturation models [34, 35], and appear to scale with projectile momentum fractions, x_1, rather than with the target fraction x_2.

While the most recent PHENIX data [36] seem to exhibit a stronger than linear impact parameter dependence of shadowing [37], the min bias results for $R_{\rm dAu}$ are in good agreement with calculations based on Ref. [15], as are the results in the most central impact parameter bin. Indeed, these new data suggest that while the shadowing may decrease more strongly than the calculations of Refs. [29, 30] predict, the strength increases rather slowly for low impact parameters.

To illustrate the effect of a larger than linear impact parameter dependence of shadowing, we compare the results for shadowing parameterizations that depend on the local nuclear matter density and on the parton path length through nuclear matter [30],

$$S^i_\rho(A, x, Q^2, \vec{r}_T, z) = 1 + N_\rho(S^i(A, x, Q^2) - 1)\left(\frac{\rho_A(\vec{r}_T, z)}{\rho_0}\right)^n , \tag{5}$$

$$\begin{aligned} S^i_{T_A}(A, x, Q^2, \vec{r}_T, z) &= 1 + N_{T_A}(S^i(A, x, Q^2) - 1)\left(\frac{\int dz \rho_A(\vec{r}_T, z)}{\int dz \rho_A(0, z)}\right)^n , \\ &= 1 + N_{T_A}(S^i(A, x, Q^2) - 1)\left(\frac{T_A(\vec{r}_T)}{T_A(0)}\right)^n , \end{aligned} \tag{6}$$

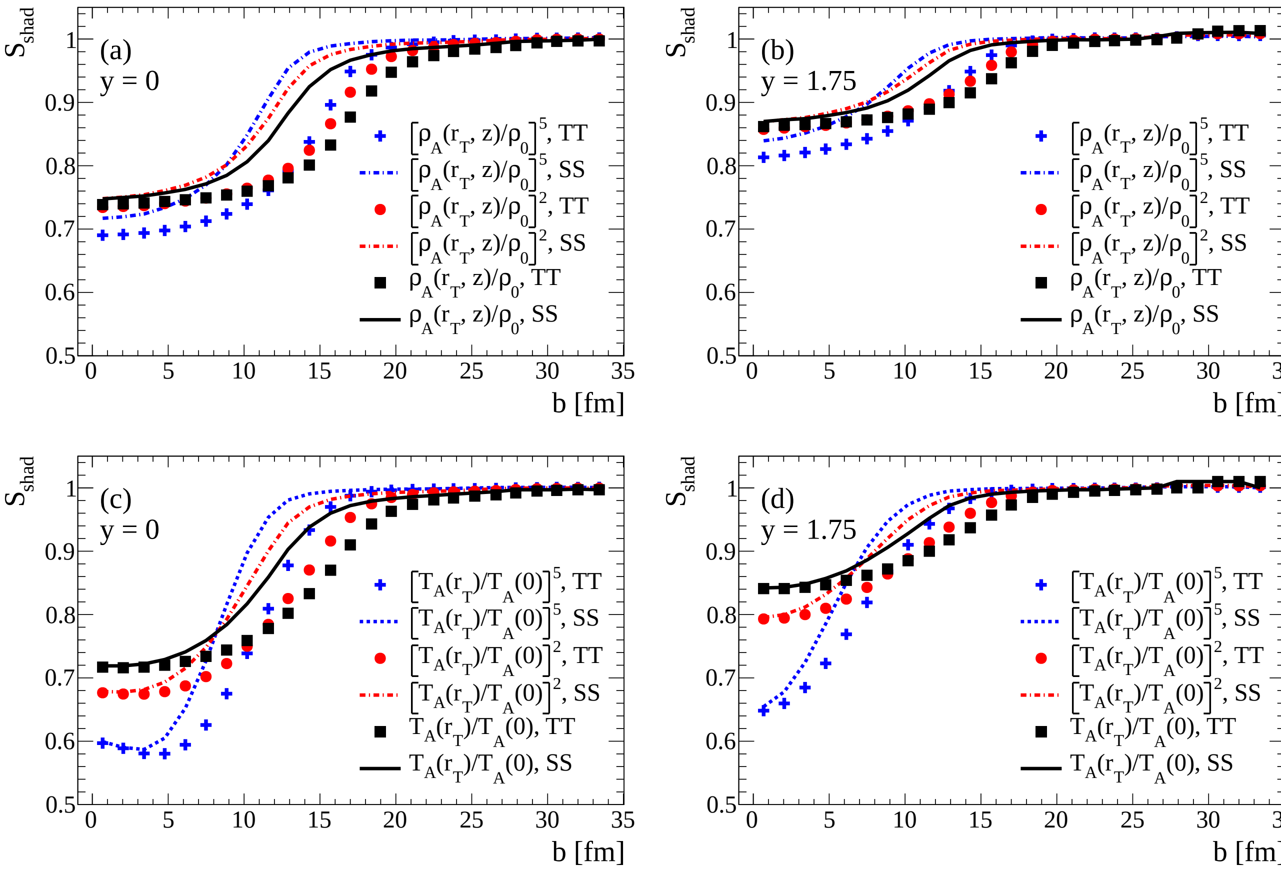

Figure 1: (Color online) The survival probability due to shadowing, $S_{\rm shad}$ in TT (lines) and SS (symbols) orientations of U+U collisions for (a),(c) $y = 0$ and (b),(d) $y = 1.75$ assuming the impact parameter dependence of shadowing is proportional to ρ (top) and T_A (bottom) for $n = 1$, 2 and 5.

where T_A is the nuclear profile function and N_ρ, N_{T_A} are chosen to normalize the integral of $S^i(A, x, Q^2, \vec{r}_T, z)$ over the nuclear volume, weighted by the nuclear density distribution, to $S^i(A, x, Q^2)$ in minbias collisions. The values of the normalizations are dependent on the power of n chosen as well as the parameterization of the impact parameter dependence. Results are shown in Fig. 1 for $n = 1$, 2 and 5.

When the shadowing is parameterized according to the nuclear density, as in Eq. (5), the difference between the TT and SS configurations is rather distinct over a broad range of impact parameters. The shape of $S_{\rm shad}(b)$ resembles the Woods-Saxon density distribution. The normalization, N_ρ, changes slowly with n. The difference between the two spatial orientations of U+U collisions, TT and SS, is very small for most central collisions, $b < 6$ fm. As n increases, N_ρ increases, as does the difference between the TT and SS orientations. Nonetheless, the results retain the general Woods-Saxon shape while impact parameter dependence steepens over the transition from shadowing to free nucleon behavior. This transition is centered around $b \sim 2R_C$ for $n = 1$, the impact parameter where the effect of shadowing is half the $b = 0$ value. Note, that $R_C = R_{\rm T}$, the length of the long axis in TT configurations, and $R_C = R_{\rm S}$ in SS configurations.

When the longitudinal direction is integrated over, as in Eq. (6), the distinctive Woods-Saxon shape seen in the upper half of Fig. 1 is somewhat washed out and $S_{\rm shad}$ increases rather smoothly with impact parameter. A separation between the TT and SS configurations is already apparent for small values of b. In this case, N_{T_A} depends more strongly on n so that the difference between $n = 1$ and $n = 2$ is larger here than for Eq. (5).

Increasing n reduces the effective radius for shadowing in both formulations in Eqs. (5) and (6). We have only shown results for $n \leq 5$ but have checked higher values of n and see that the trend continues. The separation between the TT and SS configurations for Eq. (5) increases to 10% at low b for $n = 15$ while the impact parameter dependence of $S_{\rm shad}$ more closely resembles a step function. The growth of N_ρ with n remains slow. On the other hand, with the dependence of Eq. (6), the difference between the orientations remains small, even at higher n, while N_{T_A} is a stronger function of n. Large values of n are still consistent with the PHENIX data at forward rapidity [38].

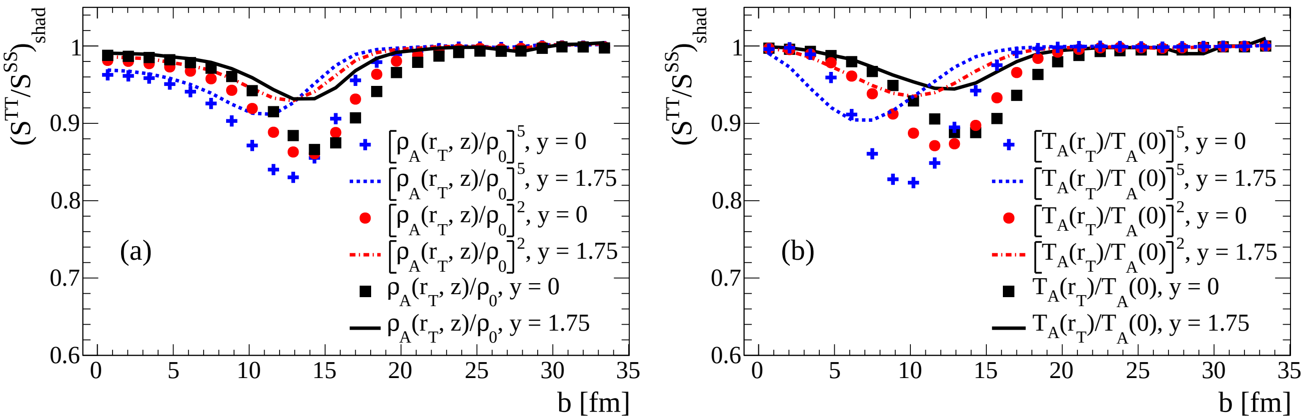

Figure 2: (Color online) The ratio of charmonium survival probabilities, $S_{\rm shad}$, in TT and SS orientations assuming the impact parameter dependence of shadowing is proportional to ρ (left) and T_A (right) for $n = 1$, 2 and 5.

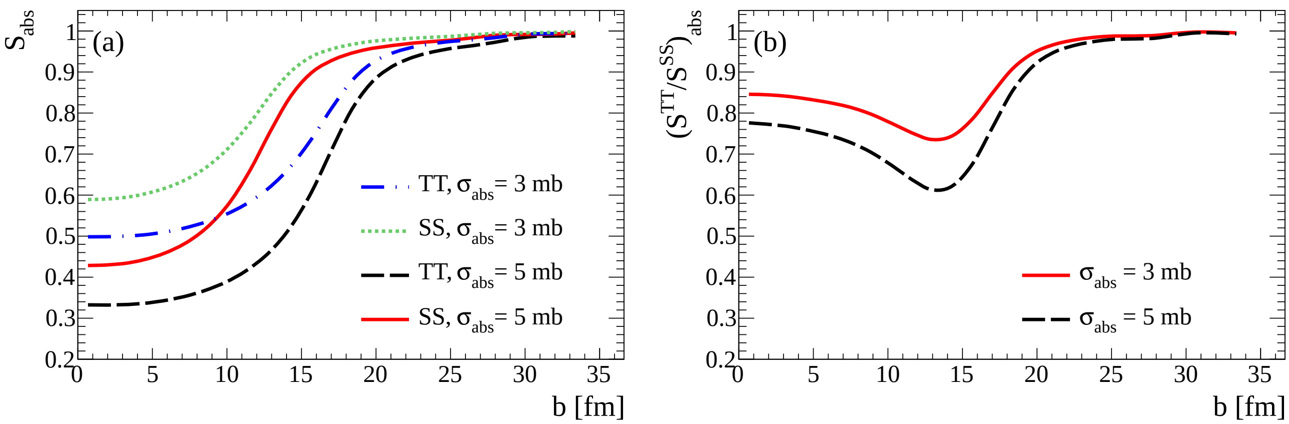

Figure 3: (Color online) (a): The J/ψ nuclear absorption survival probability, $S_{\rm abs}$, in TT and SS orientations of U+U collisions for $\sigma_{\rm abs} = 3$ and 5 mb. (b): The ratio of results in TT and SS configurations for $\sigma_{\rm abs} = 3$ (solid) and 5 (dashed) mb.

We expect that the impact parameter dependence can be characterized by other means and only show the possible range of effects here to study the sensitivity of CNM effects in U+U collisions on the impact parameter dependence of shadowing. A full analysis of the b dependence, under study in Ref. [38], is beyond the scope of this work.

The ratio of $S_{\rm shad}$ in the two configurations is shown in Fig. 2 for the same values of y and n. Away from the transition region, the ratio is relatively constant and close to unity with a maximum 5% difference employing Eq. (5) with $n = 5$. The ratio of results with Eq. (6) is much smaller at $b \sim 0$. Thus, for moderate shadowing, the ratio in central collisions is relatively insensitive to $S_{\rm shad}$. The largest change in the ratio with $n = 1$ is at $\sim (R_{\rm T} + R_{\rm S})/2$. As n increases, the dip in the ratio TT/SS deepens and shifts to lower impact parameters. The dip is deeper for $y = 0$ where the midrapidity shadowing effect is stronger. The forward rapidity effect is weaker but tends to shift to still lower impact parameters because the assumption of factorization pairs strong shadowing in one nucleus with small shadowing or some antishadowing in the other. In both cases, since $f_i^A(x, Q^2, \vec{r}_T, z)$ is proportional to the nuclear density distribution, see Eq. (1), the shape of $S_{\rm shad}(b)$ directly reflects the spatial orientations of the U nuclei.

We now discuss the impact parameter dependence of the survival probability for nuclear absorption. Figure 3 (a) shows $S_{\rm abs}$ as a function of b for U+U collisions in the TT and SS configurations assuming $\sigma_{\rm abs} = 3$ and 5 mb. These two values of $\sigma_{\rm abs}$ bracket the range obtained by the RHIC experiments. As previously discussed, the min bias result, $R_{\rm dAu}$, reported recently by PHENIX [36] is relatively well described by the EPS09 shadowing parameterization with $\sigma_{\rm abs} = 4$ mb. Before the most recent PHENIX data [36] were available, the divergence of $R_{CP}(y)$ from the calculations of absorption with shadowing was quantified the extraction of a rapidity-dependent absorption cross section [35]. These results showed a strong increase of the effective absorption cross section at forward rapidity which could be attributed to a heretofore neglected effect such as initial-state energy loss. However, a reanalysis of these data based on a more complete understanding of the impact parameter dependence of nuclear shadowing would affect the magnitude of the extracted absorption cross section. This will be addressed in Ref. [38].

While a similar trend as a function of b is observed relative to Fig. 1, the difference between TT and SS orientations at $b = 0$ is larger for absorption. Thus nuclear absorption is the only relevant orientation-dependent CNM effect in central collisions. The larger effect is due to the exponential factor in $S_{\rm abs}$, proportional to the path length, in addition to the overall dependence on the density in the calculation of the total J/ψ yield. Thus the angular orientation of the colliding nuclei affects absorption more strongly than shadowing. The exponential dependence on density in $S_{\rm abs}$ also broadens the transition region around $b \sim 2R_C$.

The ratio of survival probabilities for the two orientations is shown in Fig. 3(b) for $\sigma_{\rm abs} = 3$ and 5 mb. The ratio shows a $\sim 20\%$ difference relative to the maximum 5% for shadowing alone. It also varies more slowly with impact parameter, as seen by comparing Figs. 2 and 3(b).

Figure 4 shows the ratios of the total J/ψ survival probability in the TT and SS configurations due to cold nuclear matter effects, $S_{J/\psi} = S_{\rm abs}S_{\rm shad}$, as a function of impact parameter. In central collisions, $b < 5$ fm, the magnitude of $(S^{\rm TT}/S^{\rm SS})_{J/\psi}$ is most sensitive to $\sigma_{\rm abs}$ while at larger impact parameters, $b \geq 10$ fm, $(S^{\rm TT}/S^{\rm SS})_{J/\psi}$ is dominated by shadowing. If the TT and SS orientations could be effectively selected in an experiment, these features could help differentiate cold nuclear matter effects from color screening effects. However, the best case scenario would be to first attempt to select the tip and side orientations of the uranium nuclei in d+U collisions.

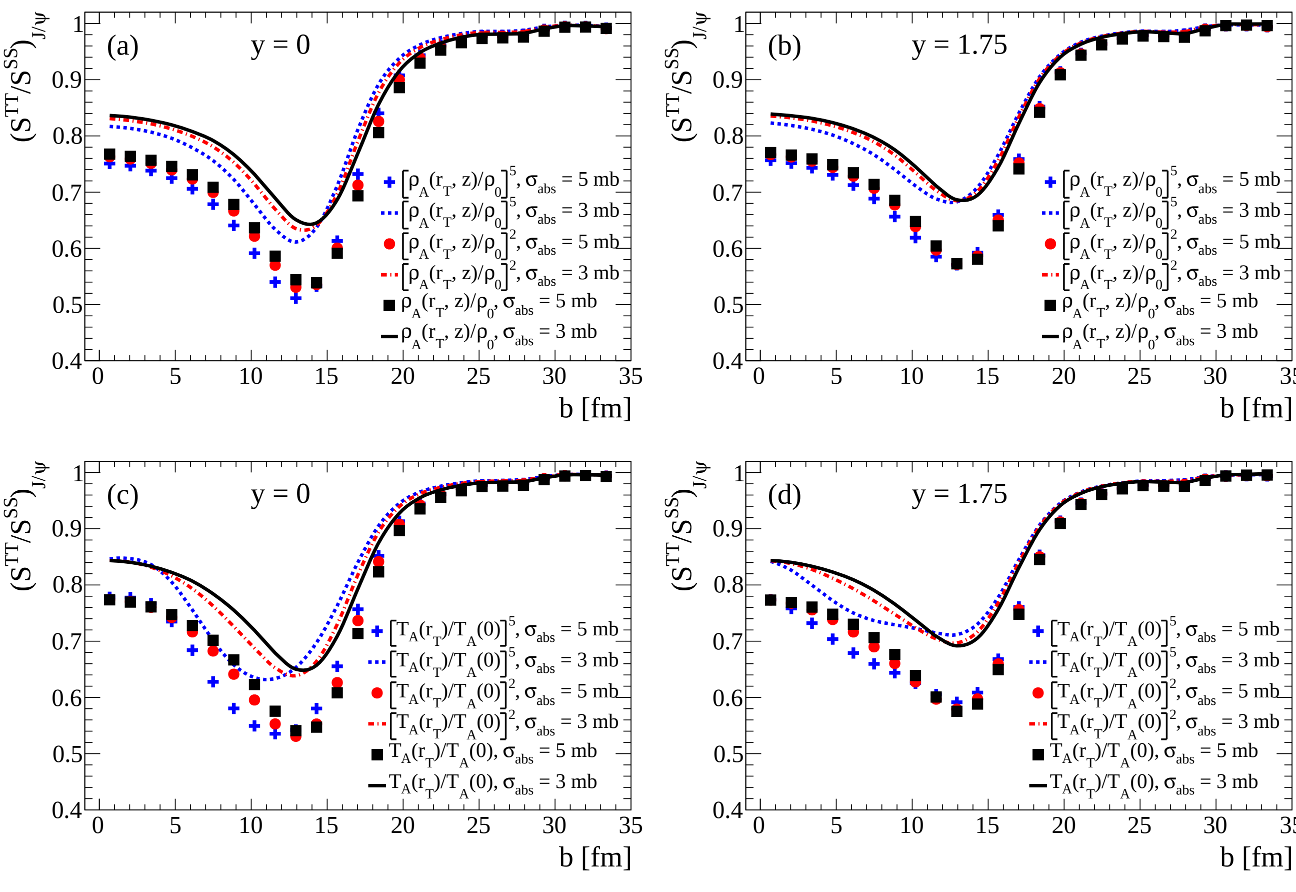

Figure 4: (Color online) The ratio of the cold nuclear matter J/ψ survival probability in TT relative to SS orientations of U+U collisions for $\sigma_{\rm abs} = 3$ and 5 mb assuming different parameterizations of the impact parameter dependence of shadowing (see text for details).

Even if the TT or SS configurations cannot be selected due to either technical difficulties or low efficiencies, U+U collisions averaged over all orientations could be used for quarkonium studies. There are no significant experimental difficulties and the nuclear path length L and charged track density are respectively 5-10% and 10-15% larger for the same centrality class in Au+Au collisions [3]. The larger L increases the effective nuclear absorption. Figure 5 shows the orientation-integrated $S_{\rm abs}$ as a function of impact parameter for Au+Au and U+U collisions with $\sigma_{\rm abs} = 3$ and 5 mb. The difference between $S_{\rm abs}^{\rm UU}$ and $S_{\rm abs}^{\rm AuAu}$ is largest $\sim 5\%$ at $b \sim 11 - 12$ fm and can be attributed to the difference in radii, 6.81 fm for uranium and 6.38 fm for gold. The magnitude of the difference depends on σ_{abs}.

On the other hand, the relative difference in the shadowing effect is negligible. The expected S_{shad} is shown in Fig. 6 for d+Au and d+U collisions (a) as well as Au+Au and U+U collisions (b). Shadowing effects in U+U and Au+Au collisions at the same $\sqrt{s_{NN}}$ are very similar at a given value of b. Thus the uncertainty due to shadowing will cancel in the ratio of the J/ψ yields in U+U and Au+Au collisions.

We now discuss the modification of Υ production in Au+Au and U+U collisions due to cold nuclear matter effects. The nuclear absorption of $\Upsilon(1S)$ seems to be significantly weaker than for J/ψ [28]. Moreover, antishadowing may be expected at midrapidity rather than shadowing, supported by the experimental results at RHIC. The cross section of Υ production in d+Au collisions is well described by the color evaporation model with antishadowing and no nuclear absorption [40]. The expected S_{shad} for Υ is shown in Fig. 7 for d+Au and d+U collisions (a) as well as for Au+Au and U+U collisions (b). The effect of shadowing is much smaller than for J/ψ. Instead, antishadowing at midrapidity may increase the Υ rate by as much as 20-30%. Note that antishadowing effects in U+U and Au+Au collisions at the same $\sqrt{s_{NN}}$ are very similar, as is the case for the J/ψ. Furthermore, a different formulation of the quarkonium production model, such as in Ref. [41], would yield similar results even though the larger average scale used in those calculations further reduces the overall shadowing effect.

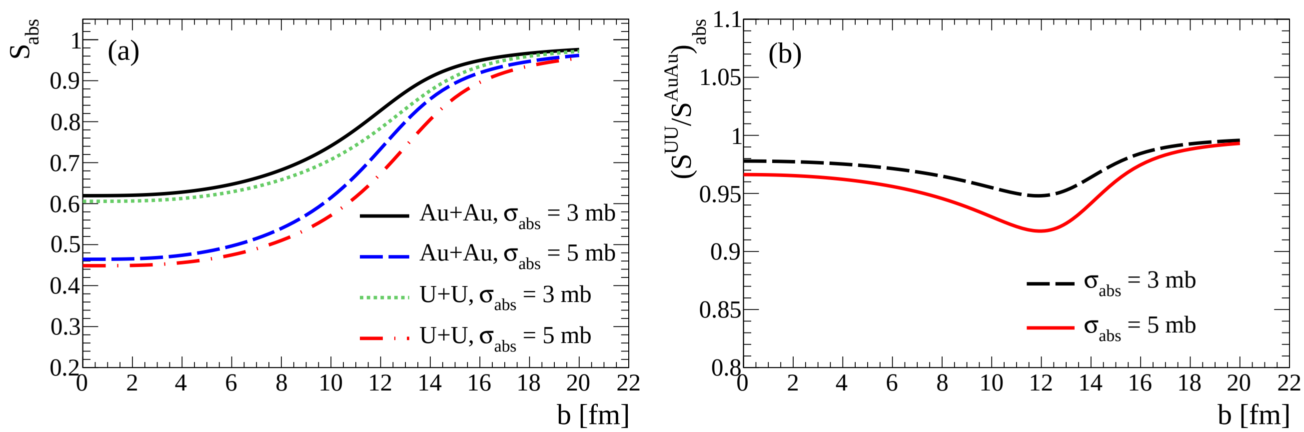

Figure 5: (Color online) Nuclear absorption as a function of b for Au+Au and U+U collisions averaged over all orientations (a) and the ratio of U+U relative Au+Au collisions (b).

Finally, we comment on the suggestion that double-color filtering and mutual boosting of the saturation scales in colliding nuclei make the transition of cold nuclear matter effects from pA to AA collisions nontrivial [33]. However these effects are rather small at RHIC energies (less than 10% for double-color filtering and 18% for mutual boosting of the saturation scales). In addition, they act in the opposite directions, therefore canceling to a large extent. Reference [33] proposed that an increase of J/ψ p_T broadening in AA collisions relative to pA would directly reflect the boosting effect. Such an increase is not seen at RHIC. In fact, $\langle p_T^2 \rangle$ at midrapidity in Au+Au collisions at $\sqrt{s_{NN}}$ = 200 GeV is approximately independent of centrality [39]. Determining the nature and strength of such a boosting effect at RHIC requires high precision data. Moreover, the effects proposed in Ref. [33] will be very similar in Au+Au and U+U collisions and thus cancel if ratios of J/ψ production in the two systems are studied.

IV. ENERGY DENSITY AND TEMPERATURE IN U+U COLLISIONS

We now investigate what energy densities and temperatures are accessible in U+U collisions. The charged track density is expected to increase in U+U interactions compared to Au+Au. Therefore, the U+U temperature should be higher in the deconfined phase. Employing U+U collisions could extend the range of temperatures accessible at RHIC and test the sequential melting hypothesis of charmonium and bottomonium states. Suppression of $\Upsilon(1S)$ beyond CNM effects would constitute direct proof of color screening since secondary Υ production by coalescence from a QGP is negligible at RHIC. Comover absorption is also insignificant. Recent STAR results show that the $\Upsilon(1S)$ is not strongly suppressed in central Au+Au collisions [42]. Below, we investigate whether the temperature of the matter produced in U+U collisions could be high enough to expect "melting" of the $\Upsilon(1S)$ state in addition to J/ψ suppression.

We use the Bjorken formula [43] to estimate the energy density available in U+U collisions. The Bjorken energy

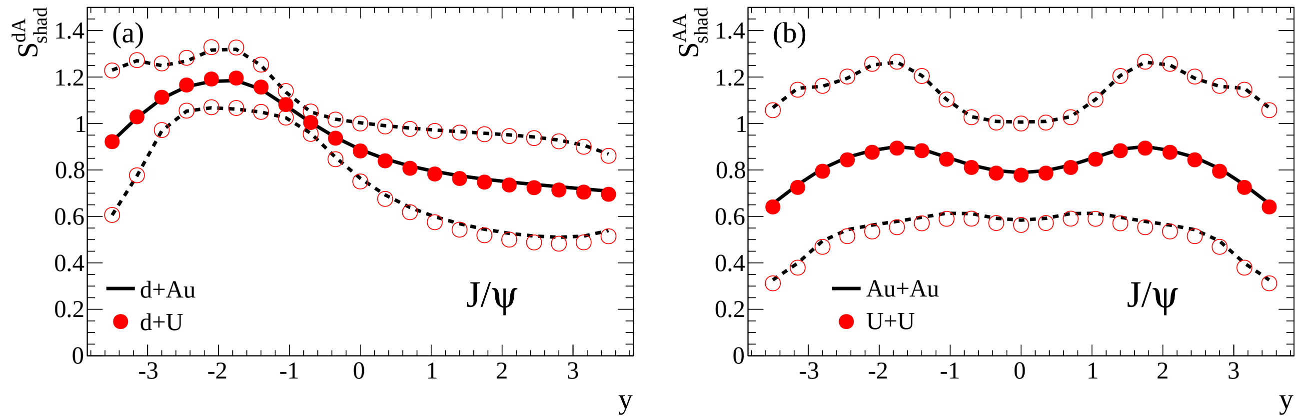

Figure 6: (Color online) The J/ψ survival probability due to shadowing in d+A (a) and $A+A$ (b) collisions. The solid lines (filled circles) represent results for Au (U) nuclei obtained with the central EPS09 shadowing parametrization while the dashed lines (open circles) show the results with the upper and lower limits of the EPS09 uncertainty.

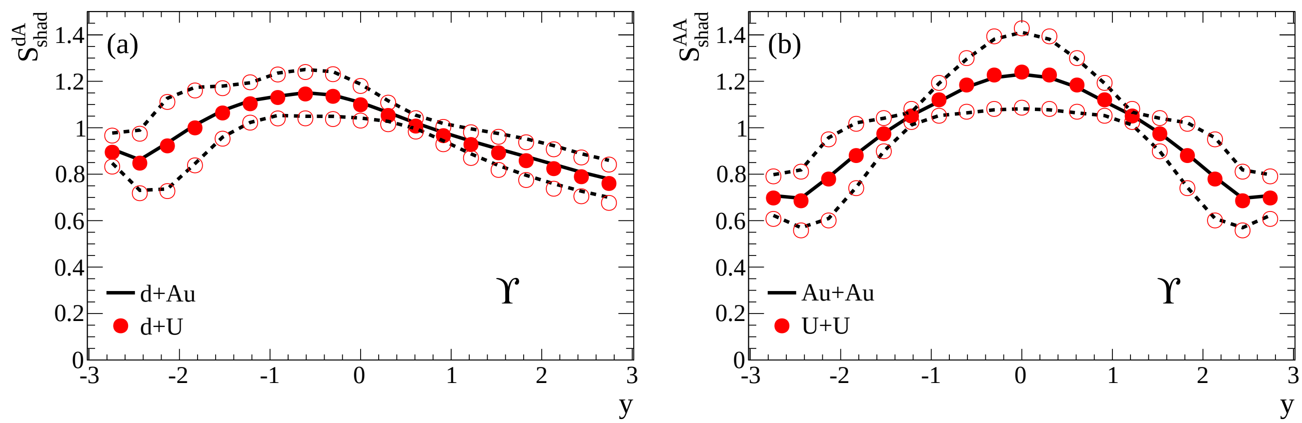

Figure 7: (Color online) The Υ survival probability due to shadowing in d+A (a) and $A+A$ (b) collisions. The solid lines (filled circles) represent results for Au (U) nuclei obtained with the central EPS09 shadowing parametrization while the dashed lines (open circles) show the results with the upper and lower limits of the EPS09 uncertainty.

density in a one-dimensional longitudinally expanding system can be calculated using

$$\epsilon_{\rm B} = \frac{1}{\tau S_\perp} \frac{dE_{\rm T}}{dy} \tag{7}$$

where τ is the formation time of the medium, $S_\perp$ is the transverse area overlap of the colliding nuclei, and dE_T/dy is the transverse energy density. We estimate dE_T/dy from PHENIX data [44],

$$\frac{dE_T}{dy} = C_{\eta\to y} \frac{E_T}{N_{\rm ch}} \frac{dN_{\rm ch}}{d\eta} \ , \tag{8}$$

where $E_T/N_{\rm ch} \equiv \langle dE_T/d\eta\rangle/\langle dN_{\rm ch}/d\eta\rangle$ is the average transverse energy density per charged track and $C_{\eta\to y} = 1.25\pm0.05$ is a scale factor converting $dE_T/d\eta|_{\eta=0}$ to $dE_T/dy|_{y=0}$. In Au+Au collisions at $\sqrt{s_{_{NN}}} = 200$ GeV, $E_T/N_{\rm ch}$ is constant over a broad range of event centralities (0-60%). We assume that $(E_T/N_{\rm ch})_{\rm AuAu}$ is a good approximation of $(E_T/N_{\rm ch})_{\rm UU}$.

The most important ingredient is the overlap area $S_\perp$, calculated in the Glauber framework. It depends strongly on the definition used in calculations. For example, the values of $S_\perp$ published by PHENIX [44] and STAR [45] are a factor of five larger than results calculated for U+U and Au+Au collisions in Refs. [2, 3]. When the relative differences between the energy densities of U+U and Au+Au collisions are considered, this discrepancy is unimportant as long as a consistent definition is used. However it is important when the absolute value of $\epsilon_{\rm B}$ is calculated. In this paper, we consider the case where $S_\perp$ is defined as the transverse area of the overlap zone weighted by the number of participants [2, 3]. This definition gives the effective "hot" transverse area of the overlap zone but neglects areas with low participant density, a rather small effect.

Figure 8 shows an example of the participant density profile for U+U collisions at $b = 0$ in the TT and SS configurations as well as averaged over configurations calculated in the Glauber framework of Ref. [3]. Much higher density is observed in TT compared to SS configurations as well as relative to orientation-averaged U+U collisions since the average is dominated by SS configurations [46]. Note also the narrower transverse profile of the TT configurations in Fig. 8.

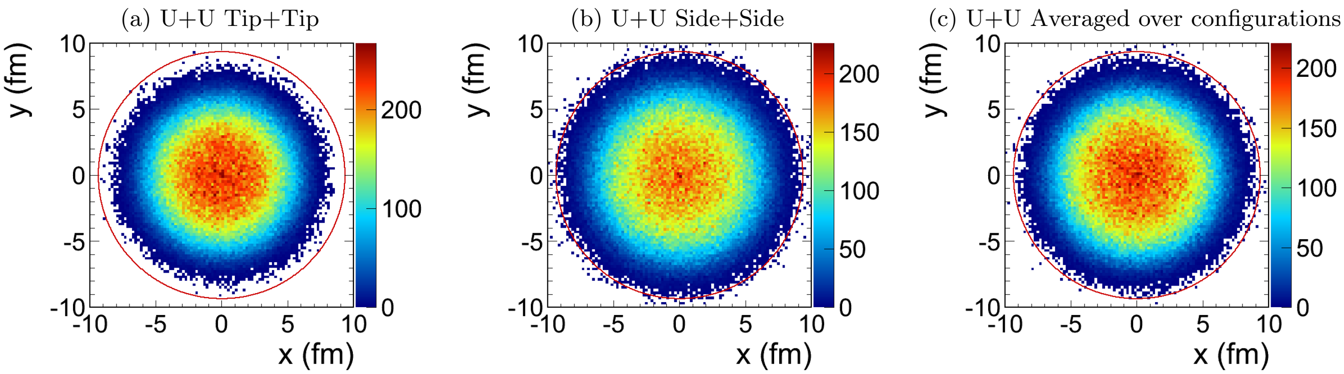

Figure 8: (Color online) Participant density profiles for U+U collisions in the TT and SS configurations as well as orientation-averaged collisions at $b = 0$. The circles are shown to guide the eye and are common to all plots [3, 46].

We use the results of Ref. [3] to estimate the increase in energy density in U+U relative to Au+Au collisions. We first estimate $\epsilon_{\rm B}$ in orientation-averaged U+U collisions. Figure 9 shows the ratio of the product $\epsilon_{\rm B}\tau$ for orientation-averaged Au+Au and U+U collisions. We note that ϵ_B is $15 - 20\%$ larger in U+U collisions relative to Au+Au collisions. Moreover, U+U collisions in the TT configuration could provide an increase of up to 30% in the charged track density, $1/S_\perp dN_{\rm ch}/d\eta$, relative to orientation-averaged collisions at the same value of b, as shown in Fig. 10(a). Since $1/S_\perp dN_{\rm ch}/d\eta$ is proportional to ϵ_B, TT configurations can thus increase $\epsilon_B\tau$ by 20-30% in central and semi-central ($b < 8$ fm) U+U collisions, as shown in Fig. 10(b).

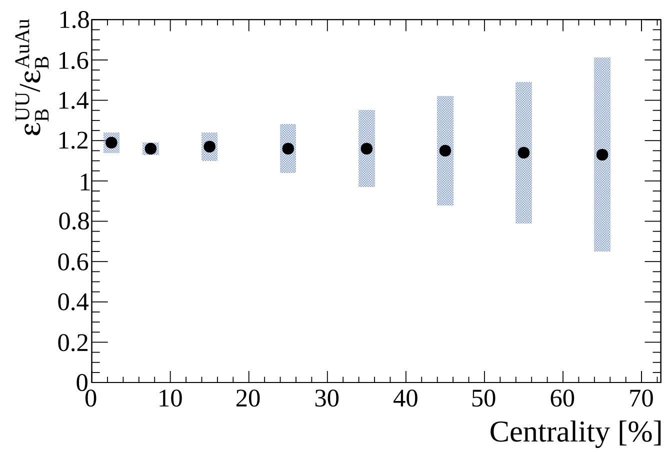

Figure 9: The ratio of Bjorken energy densities in U+U and Au+Au collisions as a function of centrality. The shaded boxes are the systematic uncertainties on $dN_{\rm ch}^{\rm UU}/dy$ and $dN_{\rm ch}^{\rm AuAu}/dy$ added in quadrature. The statistical uncertainties are negligible [3].

In our case, the relevant formation time, τ, is the time required to develop the qaurkonia wavefunction. The lower limit on the charmonium formation time is the time required for color neutralization of the $c\bar{c}$ pair, $\tau_\psi \simeq (2m_c\Lambda_{\rm QCD})^{1/2} \simeq 0.25$ fm for low p_T J/ψ [47]. The formation time of the final-state J/ψ, however, may be somewhat longer. In Ref. [14], the formation time for low p_T ground state quarkonia is estimated to be the inverse of the binding energy, $E_{\rm bind}$, $\tau \sim 1/E_{\rm bind}$. With $E_{\rm bind}^{J/\psi} = 0.64$ GeV and $E_{\rm bind}^{\Upsilon} = 1.1$ GeV [48], the formation times for the J/ψ

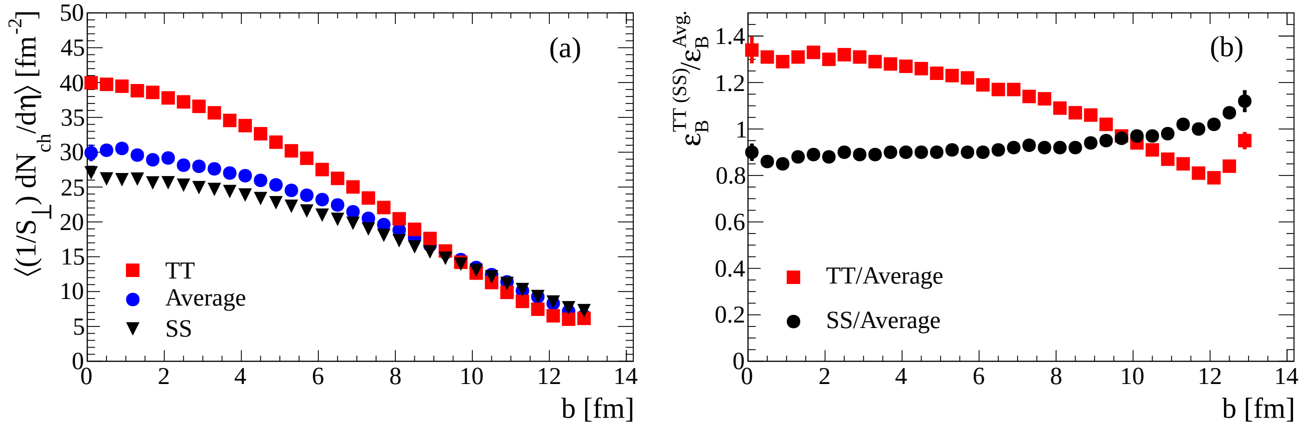

Figure 10: (Color online) (a): The average charged track density per unit of pseudorapidity η in U+U collisions in TT and SS configurations as well as orientation-averaged collisions as a function of impact parameter. (b): The ratios of energy densities in TT and SS orientations relative to orientation-averaged collisions as a function of b. In both cases, the statistical uncertainties are less than the size of the symbols.

and $\Upsilon(1S)$ are $\tau_{J/\psi} \approx 0.3$ fm and $\tau_\Upsilon \approx 0.18$ fm respectively. We used two values of τ in our studies: $\tau = 0.25$ fm to evaluate the maximum temperature relevant to J/ψ suppression due to color screening (the lower limit on the J/ψ formation time) and $\tau = 1.0$ fm, a rather conservative estimate of the time needed for the system to reach local thermal equilibrium.

We estimate the maximum energy density in $b = 0$ U+U collisions with TT orientations. In this case, $1/S_\perp dN_{\rm ch}/dy|_{y=0} \approx 43.9$ fm^{-2} while $1/S_\perp dN_{\rm ch}/dy|_{y=0} \approx 31.5$ fm^{-2} in orientation-averaged Au+Au collisions [49]. A proposed experimental method for selecting TT orientations gives $1/S_\perp dN_{\rm ch}/dy|_{y=0} \approx 40$ fm^{-2} although an effective trigger has yet to be developed [49].

In order to convert energy density to temperature and estimate T/T_c, we use lattice QCD results for $\epsilon(T)$ from Ref. [50] with $T_c \approx 185$ MeV. We find, that, for $\tau = 0.25$ fm, the temperature exceeds $2.7T_c$ in both U+U and Au+Au central collisions. However, for $\tau = 1.0$ fm, the temperature is below $2T_c$ in Au+Au collisions while it could reach $2T_c$ in central U+U collisions averaged over orientations and may exceed $2T_c$ in TT orientations, see Table I. Consequently, selecting TT configurations in U+U collisions would extend the range of temperatures accessible at RHIC to test the hypothesis of sequential quarkonium melting. The temperature in U+U TT collisions would thus be high enough to determine whether the $\Upsilon(1S)$ dissociates at $T \approx 2T_c$ [51].

Table I: The accessible temperature for $\tau = 1$ fm in the 5% most central Au+Au and U+U collisions averaged over spatial configurations, ideal TT U+U collisions and those which may be selected experimentally, TT (exp), as described in Ref. [49].

System	T [MeV]	T/T_c
Au+Au (0-5%)	351^{+9}_{-10}	1.90
U+U (0-5%)	366^{+9}_{-10}	1.98
U+U (TT, exp)	376	2.03
U+U (TT, ideal)	385	2.08

V. EXPERIMENTAL SELECTION OF TT AND SS CONFIGURATIONS

There are several strategies which can be used to select TT and SS (or TT- and SS-enriched) event samples. In general, the number of binary collisions in central and mid-central collisions in TT configurations is higher than in SS configurations at the same b, leading to higher multiplicities in TT configurations. Therefore TT-enriched head-on ($b = 0$) events could be selected by experimental cuts on the measured charged-track multiplicities. This method could be extended to other centralities. The centrality class can be established by employing Zero Degree Calorimeters (ZDCs) which measure the energy of spectator nucleons traveling in the forward and backward directions. TT-enriched events would be then selected from the centrality class by a multiplicity cut. Results obtained in Monte Carlo Glauber simulations show that the charged track multiplicity $dN_{\rm ch}/d\eta$ in central TT collisions is $\approx 17\%$ higher than central collisions in the SS configuration at $b = 0$. The difference decreases with b although $dN_{\rm ch}^{\rm TT}/d\eta$ is still 10% higher at $b = 4.5$ fm [46]. Therefore, the multiplicity difference is suitable for offline event selection. Selection of Tip and Side orientations in pU collisions would be probably more challenging because the overall multiplicity will be lower. However, the number of binary collisions in p+Tip interactions should be significantly higher than in p+Side collisions. The relative difference could be large enough for separation to be feasible in those cases.

Another approach for selecting collision orientation was proposed in Ref. [49]. TT and SS configurations have different elliptical eccentricities and, consequently, different magnitudes of anisotropic flow. The 'reduced flow vector' was proposed in addition to multiplicity cuts to select SS and TT samples with high purity.

In any case, selecting a particular collision geometry requires detailed modeling and simulations of experimental observables.

Note that, for CNM studies, high-purity samples are not required: the min-bias data are dominated by SS configurations. Thus TT-enriched samples with sufficiently longer path lengths L than min-bias collisions in the same centrality class would be appropriate for studying nuclear absorption. Experimental cuts could thus be adjusted to optimize the balance between the desirable $\langle L \rangle$ for physics and the efficiency of event selection.

VI. $R_{\rm AuAu}^{\rm UU}$: A NEW OBSERVABLE FOR J/ψ STUDIES

As shown in Sec. III, the strength of gluon shadowing is one of the largest uncertainties in the determination of cold nuclear matter effects on J/ψ production. The effects of shadowing are almost identical for Au+Au and U+U collisions averaged over impact parameter. Thus the relative uncertainty can be reduced by studying J/ψ production in U+U and Au+Au collisions within the same centrality class. As outlined in Sec. I, the J/ψ yield, $N_{\rm stat}^{J/\psi}$, produced by statistical recombination is proportional to the number of charm quarks in the system: $N_{\rm stat}^{J/\psi} \propto N_c^2$, and $N_{c\bar{c}} \propto N_{\rm bin}$, the number of binary nucleon-nucleon collisions. We define the relative nuclear modification factor $R_{\rm AuAu}^{\rm UU}$ as

$$R_{\rm AuAu}^{\rm UU} = \frac{dN_{J/\psi}^{\rm UU}/dy}{dN_{J/\psi}^{\rm AuAu}/dy} \left(\frac{N_{\rm bin}^{\rm AuAu}}{N_{\rm bin}^{\rm UU}} \right)^2 , \tag{9}$$

the ratio of J/ψ yields scaled by the number of binary NN collisions, $N_{\rm bin}^2$, in Au+Au and U+U collisions respectively. If the J/ψ's are produced by coalescence and suppression is indepedent of nuclear absorption and energy density, then $R_{\rm Au+Au}^{\rm UU} \approx 1$.

The min bias ratio $R_{\rm AuAu}^{\rm UU}$ has an advantage over R_{CP}, the ratio of the J/ψ yield in more central bins relative to that in the most peripheral bin, because $R_{\rm AuAu}^{\rm UU}$ does not depend on shadowing, see Figs. 6 and 7. As we have seen, shadowing can vary significantly between central and peripheral collisions but has a rather weak dependence on impact parameter. Indeed, if no selection is made on orientation in U+U collisions, the shadowing dependence will cancel in the ratio.

With the large data samples taken by STAR and PHENIX in 2009 and 2010 (and even larger data sets expected for RHIC II), the precision of the J/ψ yields will be driven by systematic rather than statistical uncertainties. The dominant systematic error ($\pm$10%) in pp interactions is the estimate of the integrated luminosity [52] which does not cancel between d+Au and Au+Au measurements, as seen in Ref. [36] where the systematic error on $R_{\rm dAu}$ is much larger than that on R_{CP}. In the case of $R_{\rm AuAu}^{\rm UU}$, systematic uncertainties would mostly cancel when Au+Au and U+U data are taken by the same detector.

These features of $R_{\rm AuAu}^{\rm UU}$ make it useful for testing models of J/ψ production and in-medium interactions as described in Sec. I. The dependence of nuclear absorption on b is rather small, but can be detected if large data sets are collected. Furthermore $R_{\rm AuAu}^{\rm UU}(y)$ will provide an additional test of models which reproduce $R_{\rm AuAu}(y)$.

VII. SUMMARY

We have investigated cold nuclear matter effects on charmonium production in U+U collisions. Such collisions provide an interesting opportunity to study J/ψ in-medium interactions since model-dependent uncertainties can be significantly reduced. We propose a new observable, $R_{\rm AuAu}^{\rm UU}$, which is free from some of the uncertainties associated with $R_{\rm AuAu}$ and R_{CP}. The experimental techniques for quarkonium measurements at RHIC are well established; there are abundant Au+Au data; and U+U collisions are planned at RHIC in the near future. Therefore, our proposed observable $R_{\rm AuAu}^{\rm UU}$ represents an additional, important handle on J/ψ in-medium interactions. Moreover, the energy density achievable in U+U relative to Au+Au collisions is up to $\approx$ 20% larger, extending the range of energy densities available for testing quarkonium suppression due to color screening.

Furthermore, U+U collisions would be also useful for cold nuclear matter studies at lower energies, as part of a RHIC Beam Energy Scan. Nuclear absorption is expected to be larger at lower energies [34] while there may be antishadowing of the nuclear gluon distribution rather than shadowing. Therefore cold nuclear matter effects could be tested more directly by lower energy U+U collisions.

Acknowledgments

We thank Hiroshi Masui for providing the Glauber calculations of Ref. [3]. This work was performed under the auspices of the U.S. Department of Energy by Lawrence Livermore National Laboratory under Contract DE-AC52-07NA27344 (RV), by Lawrence Berkeley National Laboratory under Contract DE-AC02-05CH11231 (GO and DK) and was also supported in part by the National Science Foundation Grant NSF PHY-0555660 (RV).

[1] U. W. Heinz and A. Kuhlman, Phys. Rev. Lett. **94**, 132301 (2005).
[2] C. Nepali, G. Fai and D. Keane, Phys. Rev. C **73**, 034911 (2006)
[3] H. Masui, B. Mohanty and N. Xu, Phys. Lett. B **679**, 440 (2009).
[4] T. Hirano, P. Huovinen and Y. Nara, Phys. Rev. C **83**, 021902 (2011).
[5] S. A. Voloshin and A. M. Poskanzer, Phys. Lett. B **474**, 27 (2000).
[6] B. I. Abelev *et al.* (STAR Collaboration), Phys. Rev. C **77**, 054901 (2008).
[7] P. F. Kolb, J. Sollfrank and U. W. Heinz, Phys. Rev. C **62**, 054909 (2000).
[8] T. Matsui and H. Satz, Phys. Lett. B **178** (1986) 416.
[9] M. C. Abreu it et al. (NA50 Collaboration), Phys. Lett. B **410**, 327 (1997).
[10] B. Alessandro *et al.* (NA50 Collaboration), Eur. Phys. J. C **39**, 335 (2005).
[11] R. Arnaldi et al. (NA60 Collaboration), Phys. Rev. Lett. **99**, 132302 (2007).
[12] A. Adare *et al.* (PHENIX Collaboration), Phys. Rev. Lett. **98**, 232301 (2007).
[13] L. Kluberg and H. Satz, arXiv:0901.3831 [hep-ph].
[14] R. Rapp, D. Blaschke and P. Crochet, Prog. Part. Nucl. Phys. **65**, 209 (2010).
[15] R. Vogt, Phys. Rev. C **71**, 054902 (2005).
[16] K. J. Eskola, H. Paukkunen and C. A. Salgado, JHEP **0904**, 065 (2009).
[17] B. Alessandro *et al.* (NA50 Collaboration), Eur. Phys. J. C **33**, 31 (2004); ibid. **48**, 329 (2006).
[18] M. J. Leitch *et al.* (E866 Collaboration), Phys. Rev. Lett. **84**, 3256 (2000).
[19] R. Vogt, Nucl. Phys. A **700**, 539 (2002).
[20] F. Karsch, D. Kharzeev and H. Satz, Phys. Lett. B **637**, 75 (2006).
[21] S. Gavin and R. Vogt, Nucl. Phys. B **345**, 104 (1990).
[22] R. Vogt, Phys. Rept. **310**, 197 (1999).
[23] A. Capella, L. Bravina, E. G. Ferreiro, A. B. Kaidalov, K. Tywoniuk and E. Zabrodin, Eur. Phys. J. C **58**, 437 (2008).
[24] W. Cassing, E. L. Bratkovskaya, and S. Juchem, Nucl. Phys. A **674**, 249 (2000).
[25] R. L. Thews and M. L. Mangano, Phys. Rev. C **73**, 014904 (2006).
[26] A. Andronic, P. Braun-Munzinger, K. Redlich and J. Stachel, Phys. Lett. B **571**, 36 (2003); A. P. Kostyuk, M. I. Gorenstein, H. Stöcker and W. Greiner, Phys. Rev. C **68**, 041902 (2003).
[27] A. D. Frawley, T. Ullrich and R. Vogt, Phys. Rept. **462**, 125 (2008).
[28] R. Vogt, Phys. Rev. C **81**, 044903 (2010).
[29] V. Emel'yanov, A. Khodinov, S. R. Klein and R. Vogt, Nucl. Phys. A **661**, 649 (1999).
[30] S. R. Klein and R. Vogt, Phys. Rev. Lett. **91**, 142301 (2003).
[31] R. Vogt, Heavy Ion Phys. **25** (2006), 97.
[32] D. Kharzeev, E. Levin, M. Nardi and K. Tuchin, Nucl. Phys. A **826**, 230 (2009).
[33] B. Z. Kopeliovich *et al*, Phys. Rev. C **83**, 014912 (2011).
[34] C. Lourenco, R. Vogt and H. K. Woehri, JHEP **0902** (2009) 014.
[35] N. Brambilla *et al*, Eur. Phys. J. C **71** (2011) 1.
[36] A. Adare *et al.*, (PHENIX Collaboration) arXiv:1010.1246 [nucl-ex].
[37] J. L. Nagle, A. D. Frawley, L. A. Linden Levy and M. G. Wysocki, arXiv:1010.4534 [nucl-th]
[38] A. D. Frawley, D. McGlinchey and R. Vogt, in preparation.
[39] A. Adare *et al.* [PHENIX Collaboration], Phys. Rev. Lett. **101**, 122301 (2008)
[40] H. Liu (STAR Collaboration), Nucl. Phys. A **830**, 235c (2009).
[41] E. G. Ferreiro, F. Fleuret, J.-P. Lansberg and A. Rakotozafindrabe, Phys. Lett. B **680**, 50 (2009).
[42] R. Reed (STAR Collaboration), in proceedings of the 4^{th} International Conference on Hard and Electromagnetic Probes of High-Energy Nuclear Collisions (HP2010) (2010).
[43] J. D. Bjorken, Phys. Rev. D **27**, 140 (1983).
[44] S. S. Adler *et al.* (PHENIX Collaboration), Phys. Rev. C **71**, 034908 (2005) [Erratum-ibid. C **71**, 049901 (2005)].

[45] B. I. Abelev *et al.* (STAR Collaboration), Phys. Rev. C **79**, 034909 (2009).
[46] H. Masui, private communications.
[47] D. Kharzeev and H. Satz, Phys. Lett. B **366**, 316 (1996).
[48] H. Satz, J. Phys. G **32**, R25 (2006).
[49] C. Nepali, G. I. Fai and D. Keane, Phys. Rev. C **76**, 051902 (2007) [Erratum-ibid. C **76**, 069903 (2007)].
[50] A. Bazavov *et al.*, Phys. Rev. D **80**, 014504 (2009).
[51] A. Mocsy and P. Petreczky, Phys. Rev. Lett. **99**, 211602 (2007).
[52] A. Adare *et al.* [PHENIX Collaboration], Phys. Rev. Lett. **98**, 232002 (2007).